U. Walzer, T. Burghardt, R. Hendel, J. Kley. Towards a dynamical model of Mars' evolution.
In W. E. Nagel, D. B. Kröner, and M. M. Resch, editors, High Perf. Comp. Sci. Engng. '09 (HLRS),
pages 485-510. Berlin, 2010.

Towards a dynamical model of Mars' evolution

Uwe Walzer, Thomas Burghardt, Roland Hendel, and Jonas Kley

Institut für Geowissenschaften, Friedrich-Schiller-Universität, Burgweg 11,
07749 Jena, Germany, u.walzer@uni-jena.de

Summary. We present the basic conception of a new dynamical model of the thermal and chemical evolution of Mars. Therefore new enlargements of the code Terra are necessary which allow to improve the solutions of the convection differential equations with strongly varying viscosity. These enlargements have been partly tested already. We describe considerations on the chronology of the early evolution of Mars and on magma ocean solidification since they lead to a *structural* model of the *early* Mars. This is important as a starting presupposition for a *dynamical* solution of the martian evolution similar to [122] which derives the essential features of the Earth's mantle's history. At present there is no PREM[39]-analogon neither for the present time nor for the start of the solid-state creep in the martian mantle. Mars has not only a topographical and crustal dichotomy but also a chemical dichotomy. We discuss different mechanisms which could generate not only these stuctures but also an early strong magnetic dipole field that vanishes after 500 Ma at the latest. Section 7 presents recent and future numerical improvements of the code Terra. Section 8 gives results on performance and scalability.

1 Introduction

The formation of terrestrial planets occurs stepwise. However, these steps are probably not simultaneously taking place in all solar distances. The condensation of dust grains [128] is followed by the accumulation of kilometer-sized planetesimals [126, 129, 137] which is assumed to have occured in $\leq 10^4$ a at 1 AU [27]. Gravitational attraction and gas drag generate collisions of the planetesimals inducing the growth of Moon- to Mars-sized planetary embryos within 1 Ma [90, 130]. The larger terrestrial planets are formed by further collisions. The majority of Moon- to Mars-sized planetary embryos will be consumed by these collisions within 10–100 Ma [3, 24, 26, 28]. It is well-known that the Hf-W chronometry is an excellent tool to constrain the duration of the magma ocean (MO) solidification. Based on own and other papers, Kleine et al. [64] (cf. their Table 1) estimate the following Hf/W ratios in planetary materials.

Chondrites	Hf/W = 0.6 – 1.8
Bulk silicate Mars	Hf/W = 3 – 4
Bulk silicate Earth	Hf/W = 17 ± 5
Bulk silicate Moon	Hf/W = 26 ± 2
Basaltic eucrites	Hf/W = 27 ± 8

Tungsten is siderophile. In the case of Mars, W did not possess enough time to go into the core whereas, in the case of the Earth, we observe an effective removal of radiogenic ^{182}W into the Earth's core. Therefore one might guess that Mars is essentially a single leftover planetary embryo [27]. With respect to the ^{142}Nd/^{144}Nd ratio, the Earth's mantle is nearly homogeneous. This suggests a long geological history. However, Mars has a heterogeneous ^{142}Nd/^{144}Nd ratio distribution. This points to the conservation of very early differentiated silicate reservoirs. Caro et al. [25] emphasize that Mars has preserved the largest ^{142}Nd effects of all known planetary bodies. This indicates in the same direction. Therefore and for other reasons, we propose to develop firstly simple models and algorithms, later more elaborated dynamic ones for the thermal evolution and the chemical differentiation of Mars where the numerics of the more complex code will be rather ambitious. It will be based on the program Terra [122,123,125]. It is clear that Terra and similar codes are suitable only for solid-state convection. If we add certain additional equations we are able to include also the chemical differentiation in small, partially melted regions of the mantle [122].

2 Chronology of the Early Evolution of Mars

2.1 General Remarks

The determinations of the time of accretion, core formation, mantle differentiation, and MO solidification mainly stem from isotope chemistry, but partly also from relatively simple models which have not been calculated in a really *geodynamic* way. It is important to have an appropriate idea at least on the order of magnitude of these times, t. All time data given here refer to the generation of Ca, Al-rich inclusions (CAIs) at an age, τ, of 4568.3 ± 0.7 Ma [64] if not noted otherwise. The absolute age of CAIs, however, is not known exactly enough but it seems to be somewhere between 4567.11 ± 0.16 Ma [4,5] and 4568.5 ± 0.5 Ma [18]. The times of a certain process of Mars are between the times of the corresponding process of the mesosiderite parent body (MPB), of the eucrite parent body (EPB) and of the angrite parent body (APB) on the one hand and of Earth on the other hand. The accretion of MPB, EPB and APB has been largely completed within t = 0.8 Ma [17]. The *initiation* of basaltic magmatism was at 2.56 Ma for MPB, at 3.05 Ma for EPB and at 3.31 Ma for APB according to [17], where these data refer to a CAI age of τ = 4569.5 ± 0.2 Ma, or at about 3 Ma for MPB, EPB and APB according to [64]. On the other hand, the core formation of the Earth was finished to 63 % after 11 Ma according to [134] and to 63 % after about 10 Ma according to [53], Yin et al. [134] estimate the timing of core formation of the Earth at 29.5 ± 1.5 Ma using the Hf-W chronometry with a two-stage model, at 11 ± 1 Ma with a MO model. They believe that the MO segregation model is the most realistic estimate. Kleine et al. [63] determine the age for core formation on Earth at 33 ± 2 Ma. This is supplemented by [62], where they conclude from the W isotope evolution of

the bulk silicate Earth that the segregation of metal into the Earth's core cannot have ceased earlier than $t = 30$ Ma. Also at present, a general review [64] shows that the tungsten model ages for core formation in Earth range from $t = 30$ Ma to $t > 100$ Ma after CAIs. These estimations show considerably higher time values in comparison to Mars.

2.2 Accretion and Core Formation

The time of *core formation of Mars* is estimated at 1 Ma in the case of a runaway growth [28] using the isotope chronometry. In this case, a significant heating contribution by short-lived isotopes such as ^{26}Al is to be expected. Jacobsen [56] derived a martian core formation age of 3.3 Ma. Kleine et al. [61] concluded an age of 12 ± 5 Ma using Hf-W evidence from martian meteorites. Instantaneous martian core formation timescales range from 0 to 10 Ma due to uncertainties in the Hf/W ratio of the martian mantle [85]. Metallic core formation in Mars is constrained to $t = 7 - 15$ Ma from Hf-W chronometry on SNCs according to [45]. Summarizing we conclude that the martian core formation is very little constrained and that its t is somewhere between 0 and 20 Ma [64] but in any case *considerably* below the t of the Earth's core formation.

If the main part of *Mars* evolved already as a planetary embryo, we have to expect a time of $0.1 - 1$ Ma for its accretion [27]. This is the result of a computer modeling of the collisions and gravitational interactions between planetesimals. Ghosh et al. [50] propose that Mars accreted 3 Ma after CAI formation. That time is necessary to account for a deep martian MO. Hf/W chronometry: For a two-stage model, Mars reached 90% of its final mass at $t = 6$ Ma. For another model, $t = 20$ Ma is possible for completion of 90% of martian accretion. A runaway growth would lead to 1 Ma [53]. Hf-W chronometry cannot currently distinguish between the mentioned scenarios of *martian accretion* [64].

2.3 The Magma Ocean Solidification of Mars

This process is influenced by the solidus as a function of depth in relation to the adiabatic temperature as a function of depth. Although a crust is evolving soon at the surface it will be quickly subducted into the liquid MO. Because of the different slopes of the two curves, the MO freezes essentially from below. Mg-silicates are enriched in the solid layer which develops just above the core-mantle boundary (CMB). Iron- and incompatible-element rich fluid silicates dominate more and more in the remaining MO above the solid mantle. So, a gravitationally instable chemical layering evolves which causes a Rayleigh-Taylor (R-T) overturn by solid-state creep after solidification. According to the model by Elkins-Tanton [40], these two processes occur in the first 5–10 Ma of the existence of Mars. The process of martian mantle solidification alone is 98% complete in less than 5 Ma if we presuppose small initial volatile contents (0.05 wt% H_2O, 0.01 wt% CO_2). [So, this estimate takes already into account the influence of an early dense martian atmosphere.] For a low-volatile martian MO, however, this 98%-solidification occurs in less than 0.1 Ma. An earlier estimate [41] for the 98% martian MO solidification is 0.1 Ma, evidently without taking into consideration the effects of volatiles. Taking into account the

atmosphere, Zahnle et al. [138] determined the final cooling of MO to 300 °C as about 5 Ma.

This MO process could admittedly be protracted by later impacts. This is the reason why Debaille et al. [35] think about a duration of martian MO of about 100 Ma. They applied the short-lived [$t_{1/2}$ = 9 Ma] ^{146}Sm–^{142}Nd and the long-lived [$t_{1/2}$ = 106 Ga] ^{147}Sm–^{143}Nd chronometer to a suite of shergottites. Kleine et al. [64] show that there is an essential ϵ^{182}W-difference between nakhlites (N) and Chassigny (C) on the one hand and the shergottites (S) on the other hand. According to ϵ^{142}Nd, shergottites show an additional division into three groups. Therefore the early martian mantle differentiation must have taken place earlier than 60 Ma. The time of the differentiation of the NC source has been estimated at $t = 40 \pm 18$ Ma [25, 45]. *It is evident that there is a certain discrepancy between the isotope chronometry and the mineralogical and physical modeling. This problem is to be solved.*

3 The Generation of the Dichotomy of Mars

3.1 Observational Constraints

Mars shows a distinct *bipartition of its surface* into heavily cratered southern highlands and relatively smooth northern lowlands which cover about 42% of Mars' surface. The histogram with respect to percentage of surface area of the topography, i.e. the hypsometric curve, has two distinct maxima in a distance of 5.2 km [100, 127]. This difference has the same order of magnitude which we obtain for the hypsometric curve of the Earth.

The martian *crustal thickness* [81, 127] histogram has also two clear peaks, the difference of which amounts to 25 km. Unfortunately there are no seismometers on Mars up to now. Therefore there are no *seismic* determinations of the crustal thickness. That is why but also for an exact determination of the core-mantle-boundary (CMB) depth and other structural features, it is extremely important to promote the installation of broad band seismometers on Mars [71]. The previous determinations of the martian crustal thickness are based on inversions of free-air gravity, geoid and topography [81, 82, 131, 144], on considerations on the movement of inertia [15, 103], and on mass-balance constraints [117, 131]. According to [131] the martian crust is between 33 and 81 km thick where the smaller thicknesses belong to the northern plains. Nimmo [82] estimates the span of martian elastic thicknesses to values between 37 and 89 km whereas Hoogenboom and Smrekar [55] derive values between only 10 and 25 km for the elastic thickness *of the northern lowlands*. Assuming crustal densities between 2700 and 3400kg/m^3, Belleguic et al. [10] derive thickness values between 30 and 90 km for the whole martian crust. The cumulative frequency curves of the quasi-circular-depression (QCD) population of the northern plains have the same distribution as the curves of the southern-highlands population. Some authors deduce from it that the ages of the northern and southern units of the dichotomy might be equal. If this conclusion would be *exactly* true we run into difficulties regarding the generation of the magnetic stripe anomalies of the southern highlands [31]. These stripes are considerably broader (about 10°) than the magnetic anomalies which run parallel with the mid-oceanic ridges of the Earth. The variations in the crustal magnetic field of Mars show an association with major

faults of the martian highlands crust [31]. In the northern lowlands, however, the remanent crustal magnetism of the early Noachian is only hardly to distinguish. It is entirely missing in Hellas, Argyre, Isidis, Utopia and also in the younger Tharsis region. Therefore Stanley et al. [112] try to prove the possibility of a single-hemisphere dynamo. Perhaps it would be more natural to try to prove that the age of the northern lowlands is somewhat smaller than that of the southern highlands. Although the areal QCD density of the lowlands has the same order of magnitude as that of the southern highlands, it is lower than that of those parts of the highlands that include highland QCDs [46, 47, 127]. Therefore the northern lowlands crust seems to be somewhat younger than the southern highlands crust [46, 47, 127].

There is also a *chemical dichotomy* of the martian crust. The dominant type is probably rich in silica, aluminum, and the main heat-producing elements, namely U, Th and K. It has a relatively low density. The second type is a dense basalt [87] which resurfaced large portions of the northern plains. Up to now it is not clear whether the insinuated chemical dichotomy refers only to the crust. Bennett et al. [11] speculate whether the *Earth's* mantle could be laterally different regarding the chemical composition in spite of 4500 Ma of thermal convection. There are contemporaneous Greenland and Australian Eoarchean terranes with 35 ppm ^{142}Nd excess and 23 ppm ^{142}Nd excess, respectively. Since some authors tend to assume a lower stirring intensity for Mars in comparison to the Earth, we should not exclude such a type of model for Mars. Novel geochemical models of this kind [11] would, of course, strengthen the argumentation of [112].

Assuming that the lithosphere is laterally isotropic, Hoogenboom and Smrekar [55] investigated the admittance signature, the ratio of gravity to topography data as a function of wave number, for four areas in the northern lowlands. They found topographic power spectra similar to highlands regions. They [55] conclude that the Noachian highland and lowland basement formed at *similar* times and speculate whether the low magnetization of the lowlands is induced by demagnetization. Solomon et al. [106] also suggest that hydrothermal circulation along deep faults may have led to oxydation of magnetic carriers and a reduction in magnetization preferably in the lower-lying areas of major drainage basins. A gamma ray spectrometer has revealed the distribution of iron, thorium and potassium at the martian surface. Dohm et al. [37] suggest that the higher iron abundance in the northern lowlands is induced by solution transport in acidic brines that may have leached iron from the highlands and deposited it in the lowlands. This conclusion corroborates [106]. It could, however, also be that the lateral differences in the Fe, Th and K concentrations have a causal relation with the lateral chemical differences mentioned by [87].

3.2 Is the Martian Dichotomy Induced by Endogenic Mechanisms?

Only one item is clear up to now: Cratering evidence shows that the martian dichotomy is an ancient feature (age $\tau > 3.5$ Ga). It is probably related to crustal formation by chemical differentiation. It is not clear whether the generation of the dichotomy and the generation of the early magnetic dipole field can be traced back to the same mechanism, but it is possible.

The *first* possibility to explain the dichotomy would be the assumption that there was a degree-1 pattern of thermal convection *with plate tectonics* in the

very early times where the southern highlands crust clustered above the downwelling current. The physically necessary conditions for the possibility of the plate-tectonics mechanism on Earth and other terrestrial planets have been derived by [12, 13, 88, 113–115, 118, 124]. Sleep [99] was presumably the first one who proposed an early martian plate tectonics. Nimmo and Stevenson [86] thought that martian plate tectonics took place for the first 500 Ma and caused an increased surface heat flow especially above the northern lowlands. This again augmented the core heat flow and produced an episodically reversing magnetic dipole field for the first 500 Ma. However, they did not propose any explanation for the cessation of martian plate tectonics. Lenardic at al. [68] also proposed early martian plate tectonics. They believe that the end of this plate-producing mechanism is a natural consequence of the growth of the southern highlands. Also Breuer and Spohn [22] and Spohn [109] discuss the possibility of early plate tectonics on Mars. The early liquid water ocean seems to be a presupposition for plate tectonics on Mars [8]. Fairén and Dohm [43] assume a potential plate-tectonic phase in the Early to Middle Noachian. This hypothesis based on the observation that the basement of the northern lowlands is younger than the basement of the southern highlands, but older than the material exposures on the cratered highlands. Parts of the highlands crust are highly magnetized [31] so that the lowlands basement probably postdates the shut off of the dynamo. The northern plains show various episodic flood inundations and more than one ocean as a function of time [37, 44].

A *second* possibility for the production of the martian crustal dichotomy by an endogenic mechanism is a degree-1 mantle convection *without plate tectonics*. This kind of convection is generated by *strong radial viscosity variations* [75, 94, 136, 143].

A *third* possibility is a *superplume* induced by destabilization of a lower thermal boundary layer [59]. This but also other enumerated proposals could be connected with large flood basalts in the northern plains. All possibilities, up to now mentioned in Subsection 3.2, are based on the finding that subsolidus martian mantle convection is an essential prerequisite for an appropriate numerical estimation of the thermal evolution of Mars [97].

A *fourth* possibility is a *Rayleigh-Taylor overturn* after early magma ocean crystallization.

3.3 Is the Martian Dichotomy Caused by Impact(s)?

It is rather uncontested that the Utopia, Acidalia, and Chryse quasi-circular depressions are generated by an impact. Furthermore, the Tharsis region is not representative for the northern plains [81]. Therefore there have been early proposals that the northern basin was produced by a giant impact [132] or a series of multiple impacts [48]. Already early McGill and Squyres [74] disputed the multiple-impact hypothesis since it is improbable that the impacts prefer one hemisphere because of Mars' rotation. Andrews-Hanna et al. [6] investigated the MGS mission and found an elliptical northern basin if the younger Tharsis additions are stripped off. The present-day irregular boundary will become quite elliptical in this way measuring about 10,650 by 8,520 km, centered at 67° N, 200° E. Marinova et al. [73] model impacts with energies of (3-6)$*10^{29}$ J, at low impact velocities (6-10 km/s) and oblique impact angles (30-60°) which generated structures similar in size and ellipticity of the martian lowlands basin. We want to check also this option especially regarding subsequent hydrodynamic and thermodynamic mechanisms. Admittedly we should

expect that a high mountain rim is generated by the impact at the margin of the northern basin. There is no trace to be seen of it now. Can erosion explain the non-existence of the rim? Nimmo et al. [84] used a high-resolution, 2D, axially symmetric hydrocode to model vertical impacts. It is to be expected that it is not possible to obtain the elliptic form of the corrected [6] basin. Melosh [76] summarizes the recent contributions to the giant impact hypothesis. He concludes, however, that all these recent studies are not the last word on the impact origin of the Borealis basin.

4 Interior Structure Models

We explain in Section 6.2 why structural models of Mars are important as a presupposition to be able to calculate a *dynamic* martian evolution model using the code Terra since there are no shell models of Mars based on measured seismic data. Early martian structural models have been presented by [16, 72, 98]. Sohl and Spohn [103] proposed two end-member structural models: The first one was optimized to satisfy chemical SNC data whereas the second model was optimized to fulfill the *polar* moment of inertia factor. Spohn [108] reviewed the principles which are necessary to derive the internal structure of a solid-state planet. Sohl et al. [102] emphasized that the *mean* moment of inertia is required for constructing spherically symmetric structure models and used a mean moment-of-inertia factor of $I/M_P R_P^2 = 0.3635 \pm 0.0012$. They derived crustal-thickness–relative-core-radius curves for different mantle densities,ρ_m, molar magnesium numbers, Mg/(Mg+Fe), and magnesium-to-silicon ratios, Mg/Si. Zharkov and Gudkova [139] calculated similar multitudes of martian structural models, however, with more complex assumptions. Zharkov et al. [140] refined these models abandoning the spherical symmetry and using mainly new results of Konopliv et al. [65]. Verhoeven et al. [119] derive structural models of Mars combining electromagnetic, geodetic and seismic properties of the relevant materials. Their one-dimensional models depend on eight parameters: crustal thickness, crustal mean density, bulk volume fraction of iron in the mantle, olivine volume fraction of the mantle, pressure gradient, temperature profile, core radius, core mass. They select eight models fitting the observational data.

5 Tectonic Episodicity

The tectonic activities of Earth and Mars are very differently distributed as functions of time. The observations on *Earth* show an episodic continental growth [30, 60] which is distributed over the whole time axis. The integrated activity declines, but only slowly. Parman [89] showed that not only the production peaks of terrestrial ocean island basalts (OIB) but also those of the terrestrial mid-oceanic ridge basalts (MORB) can be correlated to the zircon-age peaks. These observations argue for episodic mantle melting and crustal growth on Earth. We [121, 122, 125] developed numerical models to explain the mechanism behind these terrestrial observations. The bulk of the *martian* crust formed, however, about 4.5 Ga ago, presumably from a magma ocean [87]. Later additions to the martian crust were volumetrically minor. Dohm et al. [37] observe episodes of the formation of Oceanus Borealis which took

place very early though. Nevertheless, the geologic history of Mars is far from static. The tectonism decreases. It becomes concentrated near the large shield volcanoes. The Tharsis volcanoes did not stay at the same place but they migrated in the earliest epochs [83, 141, 142] similar to the Pacific volcanic chains until they came to a standstill near the margin of Borealis basin. Neukum et al. [78–80] found an appearance of episodicity of martian resurfacing events at ages of 3.5 Ga, 1 to 1.5 Ga, 300 to 600 Ma and 200 Ma. So, the geologic activity in the martian crust was highly active $>$ 4 Ga ago and has strongly decreased in magnitude through time. However, this activity curve was not continuous but episodic.

6 Our New Model of Martian Evolution

6.1 Explaining Introduction

This part deals with physical and chemical considerations on the development of a *new martian stuctural model*. In contrast with the most published models of that

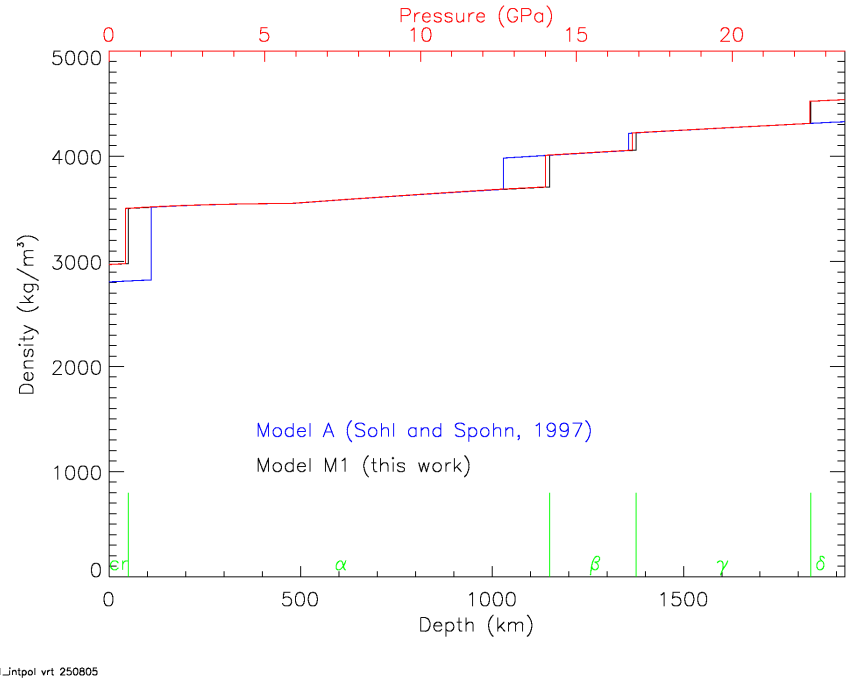

Fig. 1. A comparison of the density profile for the stuctural model [103] and our preliminary structural model of the present-day *martian* mantle. The red line refers to the pressure abscissa, the black line to the depth abscissa of our model. α, β, and γ signify the mineralogical phases of olivine. The crust is denoted by cr, a hypothetical thin perovskite layer by δ.

kind, e.g. Sohl and Spohn [103], the new model should be derived from the evolution of the martian MO. As soon as the MO is essentially solidified, our version of the code Terra is applicable, i.e, we can dynamically calculate the solid-state creep and a simplified chemical differentiation. In other words, we can solve the differential equations of the balance of momentum, energy, mass etc. similar to the method used by Walzer and Hendel [122].

Section 7 refers to *numerical improvements of the code Terra* including ideas developed in the doctoral theses [66, 77]. After the development of the new structural model of Mars, we intend to use it as an initial configuration for the newly developed Terra. We refer to Müller [77] to show that the numerical improvements are essentially more precise and comprehensive than that what we can show in this paper because of lack of space.

6.2 Towards a New Structural Model of the Early Mars

There is no seismic model of the martian mantle based on direct seismic observations since there are no martian seismic stations up to now. So, we have no analogon to PREM [39] which applies for Earth and which we have used in [122]. To apply Terra, we need a PREM-analogon for Mars but also other physical quantities as the

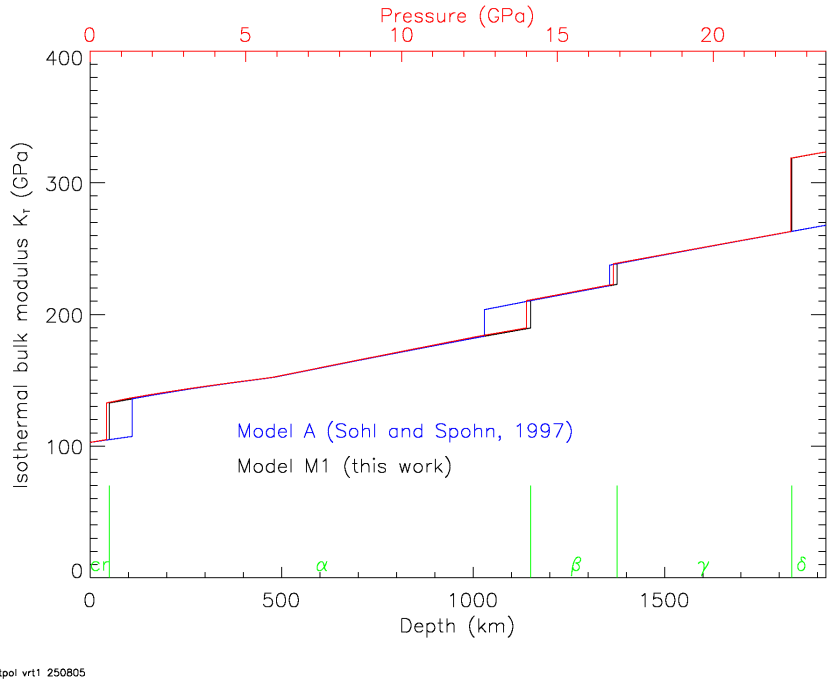

Fig. 2. A comparison of the isothermal bulk modulus profile, $K_T(r)$, for the stuctural model [103] and our preliminary stuctural model of the present-day *martian* mantle. Further remarks cf. Fig. 1.

viscosity, η, and the thermal expansivity, α, at least as a function of depth. Therefore we want to derive a chemical and mineralogical distribution model of the martian mantle similar to [103] or [52], however, not for the present time but for the time immediately after solidification of the MO and after a possible early R-T overturn.

Beforehand, different chemical models of Mars [38, 70, 96] and, if available, new chemical models should be checked and compared. With regard to core formation, the partitioning of FeO is especially important. Rubie et al. [95] have determined the partitioning of FeO between liquid iron and magnesiowüstite at pressures, P, up to 70 GPa and temperatures, T, up to 3500 K and used also data of [7] for higher pressures. If there would not appear essentially new findings, we would start, for the time being, assuming 18 wt% FeO [38] in the martian MO. For the Earth, only 8 wt% FeO are to be supposed. Even for the less realistic case of a *homogeneous* chemical distribution in the martian mantle, we need a phase diagram analogous to [57, 58], to determine the *mineralogical* layering for the solid state and to know the depths of phase transitions. In every case, the phase boundaries of [57, 58] have to be shifted in dependence on the FeO- and H_2O-abundance. The group of Falko Langenhorst works to get experimentally phase diagrams for minerals [49, 101] which are relevant for the martian mantle.

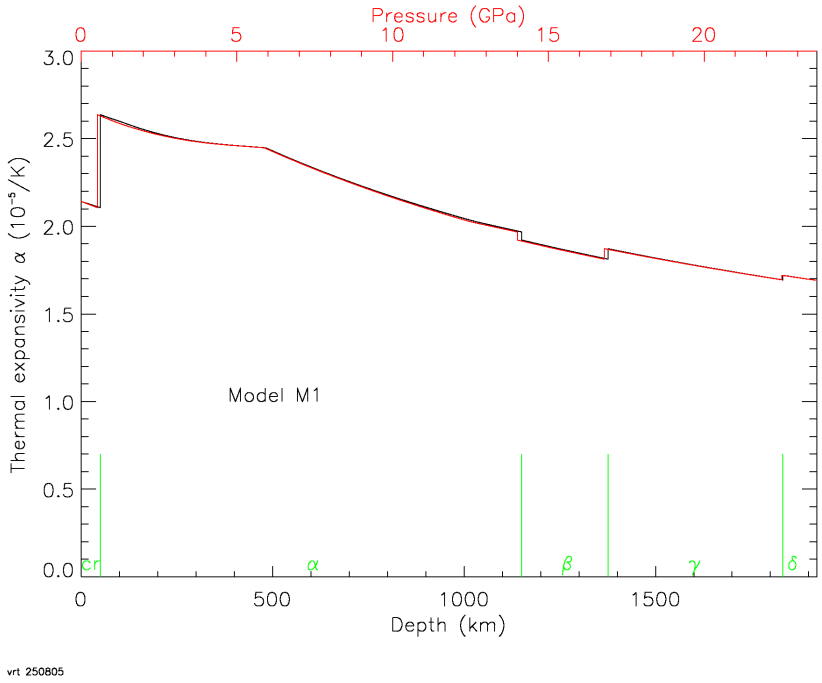

Fig. 3. The thermal expansivity, α, as a function of depth for a chemically homogeneous structural model of the present-day *martian* mantle. Further remarks cf. Fig. 1.

Walzer et al. [120] derived a *preliminary* martian structural model related to [103] and [38] assuming a chemically homogeneous martian mantle model *for the present time*. The Figures 1 to 4 show some results of this model. We do not consider these pictures as definitive but we want to improve them, especially the physical base of the derivation of Grüneisen's parameter, γ, (cf. Fig.4), and to apply the whole system to proposed chemical layerings [14, 40–42] for the temporally first solid martian silicate mantle. This solidified mantle develops after about 5 Ma according to Elkins-Tanton [14,40–42]. An unresolved question is whether we obtain a chemical layering or a compositional gradient so that the chemical composition is gradually varying as a function of radius. We want to critically test the Elkins-Tanton mechanism. As a first step, we intend to apply the physical theory to the end-member case of a chemically homogeneous martian mantle. However, from investigations of the ^{176}Lu–^{176}Hf and ^{147}Sm–^{143}Nd of shergottites, we have got evidence for a very early differentiation and a less efficient homogenization in the martian mantle [25, 36]. To check this conclusion, it is necessary to study the MO and its solidification. At first, we will start assuming an initially hot and entirely molten martian mantle which probably existed, based on geochemical evidence [20, 29, 54, 61, 93]. Kleine et al. [61] conclude from the chondritic ^{182}W/^{184}W ratio that the core-mantle-crust differentiation is constrained to 7–15 Ma.

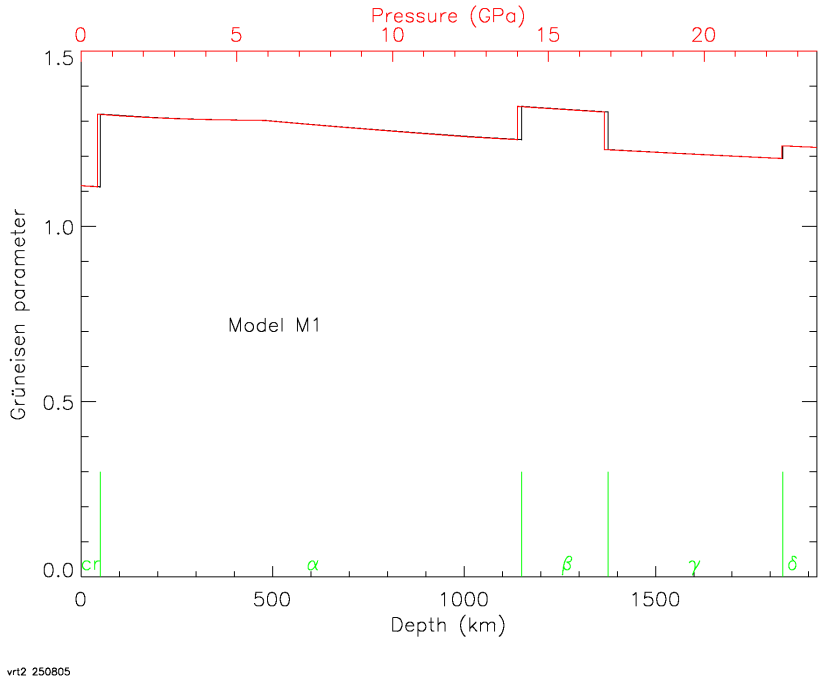

Fig. 4. The Grüneisen parameter, γ, as a function of depth for a chemically homogeneous structural model of the present-day *martian* mantle. Further remarks cf. Fig. 1.

Our actual starting point will be the model by Elkins-Tanton [40–42] which, however, is to be revised in essential, but also in minor items. But the idea is nevertheless interesting. Which part of the intended revision is the most important one is not a priori known. Here we continue some considerations of Section 2. Since it is meanwhile clear that not only the highlands but also the northern plains have a high age, it might be that the basic features of each of the two peaks in the percentage of surface area of the topography [100] and the crustal thickness [81, 127, 144] are induced by very early processes.

- Layered convection, delineated by mineral septa, is unlikely in a planetary-scale martian MO. This statement [40] seems to be right because of the high Rayleigh number of the MO. This Rayleigh number is high because, e.g., Liebske et al. [69] demonstrated that the viscosity of a synthetic peridotite liquid varies between 0.019 and 0.13 Pa·s for a pressure interval of 2.8 to 13 GPa and a temperature span between 2043 and 2523 K. The viscosity of this magma is governed by a Vogel-Fulcher-Tamman equation. So, it is non-Arrhenian. Therefore the magmatic viscosity rises as a function of pressure for $P = 0 - 8$ GPa whereas it decreases with growing pressure for $P > 8$ GPa. So, the MO is expected to be less viscous than water and to convect with high turbulence. Therefore it is very improbable that there is a chemical differentiation before the emergence of the first crystals. In spite of these arguments, we will check this conclusion by the results of [92, 104, 105].
- The solidus and liquidus curves of Longhi et al. [72] have been used in [41]. We want to replace them by new curves which are to be derived together with a new phase diagram for 18 wt% FeO as an analogon to [57, 58].
- Presumably the adiabates will be steeper than the newly derived or measured solidi, also for future phase diagrams. If so, the solid layer will grow from the CBM towards the top. Elkins-Tanton et al. [40–42] *presuppose* that the growing solid mantle *is waiting* until it touches the preliminary crust near the surface. They think that the solid-state creep begins to work not before the whole martian mantle is solidified. Furthermore they do *not dynamically* calculate the R-T overturn which comes into being by the iron enrichment of the uppermost layers of the mantle. It should be possible for us to check by the code Terra whether the solidified lower part of the martian mantle begins to flow by a R-T instability **before** the whole mantle is solidified.
- One mineralogy model has been proposed for the first solidified whole-mantle martian MO, another mineralogy model for the mantle just after the R-T overturn [40–42]. We intend to check whether these findings are appropriate if we use newer results [6] etc.
- We should be able to calculate the dynamic process of the R-T overturn by an improved Terra. We will solve the full set of differential equations which guarantees the conservation of mass, energy, momentum, angular momentum and the sums of atoms of the four most relevant radionuclides plus their corresponding daughter nuclides. Is the result really a simply reversed zero-pressure density profile given by Elkins-Tanton or is it a sequence of chemically homogeneous layers or a more complex structure?
- We can systematically vary the mineralogical assumptions and look for systematic variations in the dynamic results. Perhaps we can divide the results into classes.

- Since we observe a very early division of the mantle (cf. [64], their Fig. 10(b)) into a shergottite reservoir and a NC reservoir as well as a further division by chemical differentiation into a depleted-shergottite source (DS reservoir) with $^{180}\mathrm{Hf}/^{184}\mathrm{W} \approx 8$ and an enriched-shergottite source (ES reservoir) with $^{180}\mathrm{Hf}/^{184}\mathrm{W} \approx 2$, we should numerically solve the problem on what conditions these reservoirs are preserved until an age of 1.3 Ma, yet, and probably even until the present time.
- It is in no way evident whether the reservoir classification of the martian mantle, mentioned in the previous item, is connected with the iron enrichment in the northern lowlands. If so, then it would be an indication that the essential features of the martian dichotomy stem from the earliest history of the planet. We want to investigate if, firstly, this idea is appropriate according to observations and, secondly, if we can model it by Terra. (18–24 wt% FeO have been observed in the lowlands, 14–18 wt% FeO in the highlands. An alternative explanation is, however, the idea that the FeO-dichotomy might be due to acidic aqueous activity which could leach iron from the surface via hydrologic activity [19].) A mega-impact could be another alternative explanation of the formation of the martian crustal and chemical dichotomy [6, 46, 73, 84]. Also Watters et al. [127] think that it is most probable that the martian dichotomy evolved very early. But it is an open question whether this dichotomy came into being by one impact, by a series of impacts, or by a rapid endogenic mechanism like R-T overturn or a thermal-convection mechanism. We want to test the two last-mentioned possiblities by a Terra-based model.
- Agee [2] showed by a sink/float method that the crystal-liquid pressure dependence of density for a primitive martian melt has a crossover at $P = 9$ GPa corresponding to a martian depth of $h = 750$ km in the dry case. However, the crossover will appear deeper and deeper for increasing initial water abundance. We have to check the influence of such findings to the Elkins-Tanton FeO-distribution before and after the R-T overturn. The altered starting distribution of Fe and Mg should have different effects on the initial solid-state creep that we can calculate dynamically using Terra. The results are expected to vary with varying water abundance.
- The following item is very important. Elkins-Tanton et al. [40–42] maintain that a stable compositional stratification after the R-T overturn at $t = 5$ Ma would inhibit thermally driven convection. So, they propose that the martian mantle is perpetually resistant to thermal convection. We cannot believe it for the following reasons. Intensive East-West striking magnetic stripe anomalies have been discovered in the southern highlands [33, 34, 111]. So, the early Mars had a strong magnetic dipole field [1]. The present-day martian CMB is a solid-fluid boundary. This is a result of satellite-track investigations [135]. The orders of magnitude of the obliquity of the rotational axis and of the length of day of Mars are very similar to those of the Earth. Therefore we conclude from dynamo theory that, if the present-day temperature gradient at CMB were high enough, we should expect a strong present magnetic dipole field: The Coriolis force would bring the numerous little vortices of the fluid core into line with the rotation axis. Since the CMB heat flow is controlled by the surface heat flow we presume: The one-plate nature of the present-day martian lithosphere is the cause for the non-existence of a significant present magnetic field. On the other hand, Mars' crust is ten times more intensely magnetized than the Earth's crust.

Mars *had* an intense global magnetic field in the first few hundred Ma [1, 32]. Therefore we should expect thermally driven, probably layered martian mantle convection in those first few hundred Ma, at least, presupposed that the R-T overturn occured so quickly as mentioned above [40–42]. Of course, the present-day highly effective thermal screening is mainly caused by the thick crust and the thick lithosphere [21, 81, 107, 110].

- The previous items can only be optimally put into effect after the improvements of Section 7.

7 Numerical Improvements of Terra

Müller [77] and Köstler [66] work on improvements of Terra which, however, could not be used yet in our latest simulations. Müller analyzed the discretization of the Stokes problem and found a local grid refinement with hanging nodes which is inf-sup stable. Beate Sändig augmented the block size of the Jacobi smoother in the solver and Köstler adapted the grid transfer because of the small irregularities of the icosahedric grid. However, the influence of these alterations on the convergence behavior proved to be small. Further studies on the Krylov subspace method and multigrid method have been carried out and are continued to apply the latest results of numerical research to the Stokes solver in Terra. Especially a multigrid solver of the coupled Stokes problem, proposed by Larin and Reusken [67], should be developed to augment the convergence rates and to improve the pressure correction. We intend to implement such a solver and a MINRES procedure. As a latest result, John Baumgardner got the new free-slip boundary treatment debugged and working correctly. It is to be expected that he can move forward now on a set of benchmarks and get a Terra benchmark paper.

The computational model Terra uses a discretization of the sphere which consists of 10 diamonds evolving from the projection of the regular icosahedron onto the sphere [9]. The lateral extension of one diamond edge is an angle of about 63 degrees and the depth of this domain can be chosen arbitrarily. The size of such a segment is very appropriate to model special features of the martian crust. Because parallelization in Terra is done in lateral directions, it can be applied very efficiently to a regional domain which is a wide aspect ratio spherical shell segment. For instance on an SGI Altix 4700 machine with Intel Itanium2 Montecito Dual Core processors we could achieve an efficient cache usage with subdomains of 33x33x129 grid points which would give an overall regional grid spacing of 4 km at the surface and 3 km at the martian CMB if we use 1024 processors on one diamond with a depth of 500 km. This is 4 times less the spacing we could achieve in the whole spherical shell. Communication overhead would be much less than 10 % for this configuration. A similar approach can be done with the convection code CitComS in [116], where a 2 times finer regional grid is used.

Nevertheless, very strong gradients in material parameters, in particular viscosity, have to be taken into account. Therefore we want to further advance the Terra code with respect to stability, local grid refinement, and solver techniques. Specifically, we intend to investigate an inf-sup-stable grid modification that enables us to use grids with hanging nodes. Thus we will be able to adapt the grid resolution rapidly towards a heavily refined region with only a few successively refined layers. We will change the smoother of the multigrid solver, the preconditioner, the

algorithm for the solution of an included Stokes problem and the method of time integration. We will start refactoring the solver to achieve greater flexibility with regard to algorithm changes. We created a test framework that automates the build process, starts automatically a series of test cases on different machines in different resolutions and checks the results. This way the response time to changes and errors in the code is noticeably reduced. That means, we have facilities assisting even radical changes of the code. We can provide a fully featured parallel multigrid solver for the convection in the domain of interest, including parallel implemented tracers for chemical differentiation by a modification of the existing code (cf. Fig. 5). In addition to the adaption described, we plan to implement refined solving strategies to meet the requirements of strongly varying viscosity due to mineral phase boundaries and to differences in temperature, pressure and water content. We will use the techniques we investigated for whole mantle convection like the local grid refinement, a special preconditioning technique as well as our existing test framework. In particular, the above-mentioned preconditioned MINRES algorithm will be implemented. The benefits achieved this way would also pay off for the new dynamic martian-mantle creep model.

Having obtained a small scale method that uses essentially the same solver we have very good preconditions to integrate the small high resolution area seamlessly in the global martian convection. The spatial grid will be refined with the described technique of hanging nodes towards the boundaries of a small scale model with only a few successive refinement steps. One has however also to couple the time stepping

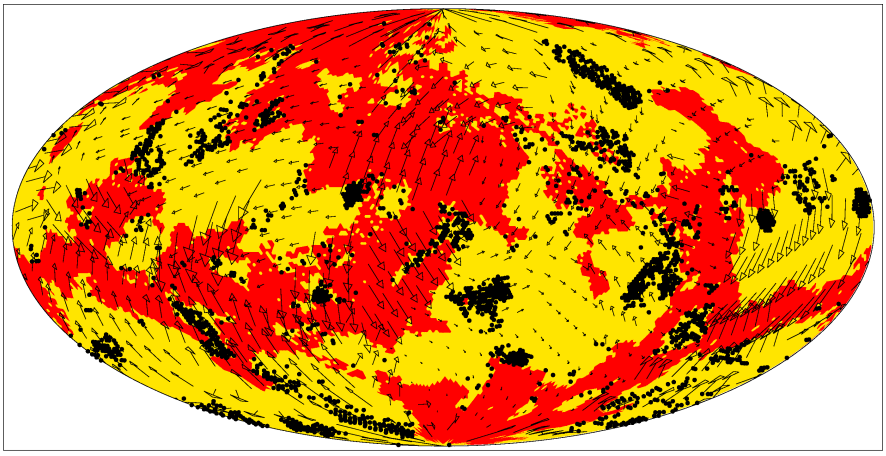

Fig. 5. A result of our convection-evolution model for the *Earth's* mantle with chemical differentiation. The tracer module used here has to be modified and strongly supplemented for the differentiation of Mars. This picture shows the distribution of continents (*red*) and oceanic plateaus (*black dots*) for the geological present of a run with yield stress $\sigma_y = 115$ MPa and viscosity-level parameter $r_n = -0.55$. The oceanic lithosphere is signified by *yellow color*.

scheme of both methods in a very flexible manner. We will have to address both, stability and optimality with respect to the load balancing. The plan to achieve these goals is simple because we do not need full adaptivity in space and time, but prescribe the spatiotemporal resolution according to optimal load balancing.

Furthermore, there exists a 2D version of Terra which can already model viscosity contrasts of up to 10^{10} between adjacent points [133]. As we use this code to study different solving strategies in two dimensions first, there is a benefit to be expected also in modeling the influences of composition and grain size. Moreover, the matrix-dependent transfer technique in the 2D code still promises an improvement of the convergence of the multigrid in the 3D code.

8 The Numerical Performance Hitherto Achieved

The Navier-Stokes equations are handled by the Finite Element Method. Pressure and velocity are solved simultaneously by a Schur-complement conjugate-gradient iteration (Ramage and Wathen, [91]). The system of linear equations is solved using a multigrid procedure in connection with matrix-dependent prolongation and restriction and with a Jacobi smoother. The temperature transport is realized by the second order Runge-Kutta method for explicit time steps.

For convergence tests we compared the results of runs with 1,351,746 and 10,649,730 nodes. The deviations concerning Rayleigh number, Nusselt number, Urey number, and the laterally averaged surface heat flow, *qob*, were smaller than 0.5 %. Benchmark tests of the Terra code (Bunge et al. [23], Glatzmaier [51]) showed deviations of less than 1.5 %.

Table 1. CPU-time, walltime and speedup for runs with 100 time steps on 1,351,746 nodes (a) and on 10,649,730 nodes (b). For comparison, Speedup (b) for 4 processors has been deliberately set to 4.00.

Procs	CPU-time (a)	Walltime (a)	Speedup (a)	CPU-time (b)	Walltime (b)	Speedup (b)
1	00:27:13	00:27:17	1			
4	00:29:12	00:07:33	3.61	05:01:23	01:16:09	4.00
8	00:26:08	00:03:31	7.76	04:53:26	00:37:32	8.12
16	00:25:36	00:02:02	13.42	05:08:51	00:19:35	15.69
32	00:21:52	00:01:02	26.40	04:34:40	00:09:11	33.17
64				05:43:25	00:05:36	54.39
128				05:34:24	00:03:04	100.42

The Terra code is parallelized by domain decomposition according to the dyadic grid refinement and using explicit message passing (MPI). In Table 1 we present measurements of scalability and performance. Using the performance measuring tool `jobperf`, we obtained an average of 1201 MFlop/s with 8 processors, 1116 MFlop/s with 32 processors, and 935 MFlop/s with 128 processors, respectively. In both resolutions the speedup was almost linear, in some cases slightly superlinear due to cache usage. With the high resolution, at least 4 processors are necessary to make efficient use of the cache memory.

Acknowledgements

We kindly acknowledge the confidential cooperation with John Baumgardner, Markus Müller, and Christoph Köstler. We acknowledge the use of supercomputing facilities at SSC Karlsruhe, LRZ München and HLRS Stuttgart. This work was partly supported by the Deutsche Forschungsgemeinschaft under the grants WA1035/5-3 and KL495/16-1.

References

1. M. N. Acuña, J. E. P. Connerney, N. F. Ness, et al. Global distribution of crustal magnetization discovered by the Mars Global Surveyor MAG/ER experiment. *Science*, 284:790–793, 1999.
2. C. B. Agee. Static compression of hydrous silicate melt and the effect of water on planetary differentiation. *Earth Planet. Sci. Lett.*, 265:641–654, 2008.
3. C. B. Agnor, R. M. Canup, and H. F. Levison. On the character and consequences of large impacts in the late stage of terrestrial planet formation. *Icarus*, 142:219–237, 1999.
4. Y. Amelin, A. N. Krot, I. D. Hutcheon, and A. A. Ulyanov. Lead isotopic ages of chondrules and calcium-aluminum-rich inclusions. *Science*, 297:1678–1683, 2002.
5. Y. Amelin, M. Wadhwa, and G. W. Lugmair. Pb-isotopic dating of meteorites using ^{202}Pb - ^{205}Pb double spike: Comparison with other high-resolution chronometers. In *37th Annual Lunar and Planetary Science Conference (abstract #1970)*. LPI, 2006.
6. J. C. Andrews-Hanna, M. T. Zuber, and W. B. Banerdt. The Borealis basin and the origin of the martian crustal dichotomy. *Nature*, 453:1212–1215, 2008.
7. Y. Asahara, D. J. Frost, and D. C. Rubie. Partitioning of FeO between magnesiowüstite and liquid iron at high pressures and temperatures: Implications for the composition of the Earth's outer core. *Earth Planet. Sci. Lett.*, 257:435–449, 2007.
8. V. R. Baker, S. Maruyama, and J. M. Dohm. A theory of early plate tectonics and subsequent long-term superplume activity on Mars. *Superplume International Workshop, Tokyo, Abstract*, pages 312–316, 2002.
9. J. R. Baumgardner and P. O. Frederickson. Icosahedral discretization of the two-sphere. *SIAM J. Numer. Anal.*, 22:1107–1115, 1985.
10. V. Belleguic, P. Lognonné, and M. Wieczorek. Constraints on the Martian lithosphere from gravity and topography data. *J. Geophys. Res.*, 110(E11):E11005, 2005.
11. V. C. Bennett, A. D. Brandon, and A. P. Nutman. Coupled ^{142}Nd - ^{143}Nd Isotopic Evidence for Hadean Mantle Dynamics. *Science*, 318:1907 – 1910, 2007.
12. D. Bercovici. Generation of plate tectonics from lithosphere-mantle flow and void-volatile self-lubrication. *Earth Planet. Sci. Lett.*, 154:139–151, 1998.
13. D. Bercovici. The generation of plate tectonics from mantle convection. *Earth Planet. Sci. Lett.*, 205:107–121, 2003.
14. C. M. Bertka and Y. Fei. Mineralogy of the Martian interior up to core-mantle boundary pressures. *J. Geophys. Res.*, 102:5251–5264, 1997.

15. C. M. Bertka and Y. Fei. Density profile of an SNC model Martian interior and the moment-of-inertia factor of Mars. *Earth Planet. Sci. Lett.*, 157:79–88, 1998.
16. A. B. Binder. Internal structure of Mars. *J. Geophys. Res.*, 74:3110 – 3118, 1969.
17. M. Bizzarro, J. A. Baker, H. Haack, and K. L. Lundgaard. Rapid timescales for accretion and melting of differentiated planetesimals inferred from ^{26}Al-^{26}Mg chronometry. *Astrophys. J.*, 632:L41–L44, 2005.
18. A. Bouvier, J. Blichert-Toft, F. Moynier, J. D. Vervoort, and F. Albarède. Pb-Pb dating constraints on the accretion and cooling history of chondrites. *Geochim. Cosmochim. Acta*, 71(6):1583–1604, 2007.
19. W. V. Boynton, G. J. Taylor, L. G. Evans, et al. Concentration of H, Si, Cl, K, Fe, and Th in the low- and mid-latitude regions of Mars. *J. Geophys. Res.*, 112:E12S99, 2007.
20. A. D. Brandon, R. J. Walker, J. W. Morgan, and G. G. Goles. Re-Os isotopic evidence for early differentiation of the Martian mantle. *Geochim. Cosmochim. Acta*, 64:4083–4095, 2000.
21. D. Breuer. Thermal evolution, crustal growth and magnetic field history of Mars. Habilitation, W. W. Univ. Münster, 2003.
22. D. Breuer and T. Spohn. Early plate tectonics versus single-plate tectonics on Mars: Evidence from magnetic field history and crust evolution. *J. Geophys. Res.*, 108(E7):5072, 2003.
23. H.-P. Bunge, M. A. Richards, and J. R. Baumgardner. A sensitivity study of three-dimensional spherical mantle convection at 10^8 Rayleigh number: Effects of depth-dependent viscosity, heating mode and an endothermic phase change. *J. Geophys. Res.*, 102:11991–12007, 1997.
24. R. M. Canup and E. Asphaug. Origin of the Moon in a giant impact near the end of Earth's formation. *Nature*, 412:708–712, 2001.
25. G. Caro, B. Bourdon, A. Halliday, and G. Quitté. Superchondritic Sm/Nd in Mars, Earth and the Moon. *Nature*, 452:336–339, 2008.
26. J. E. Chambers. Making more terrestrial planets. *Icarus*, 152:205–224, 2001.
27. J. E. Chambers. Planetary accretion in the inner solar system. *Earth Planet. Sci. Lett.*, 223:241–252, 2004.
28. J. E. Chambers and G. W. Wetherill. Making the terrestrial planets: N-body integrations of planetary embryos in three dimensions. *Icarus*, 136:304–327, 1998.
29. J. H. Chen and G. J. Wasserburg. Formation ages and evolution of Shergotty and its parent planet from U-Th-Pb systematics. *Geochim. Cosmochim. Acta*, 50:955–968, 1986.
30. K. C. Condie. Episodic continental growth and supercontinents: a mantle avalanche connection? *Earth Planet. Sci. Lett.*, 163:97–108, 1998.
31. J. E. Connerney, M. H. Acuña, N. F. Ness, G. Kletetschka, D. L. Mitchell, R. P. Lin, and H. Reme. Tectonic implications of Mars crustal magnetism. *Proc. Natl. Acad. Sci. USA*, 102:14970–14975, 2005.
32. J. E. P. Connerney, M. H. Acuña, N. F. Ness, T. Spohn, and G. Schubert. Mars crustal magnetism. *Space Science Reviews*, 111:1–32, 2004.
33. J. E. P. Connerney, M. H. Acuña, P. J. Wasilewski, et al. Magnetic lineations in the ancient crust of Mars. *Science*, 284:794–798, 1999.

34. J. E. P. Connerney, M. H. Acuña, P. J. Wasilewski, G. Kletetschka, N. F. Ness, H. Rème, R. P. Lin, and D. L. Mitchell. The global magnetic field of Mars and implications for crustal evolution. *Geophys. Res. Lett.*, 28(21):4015–4018, 2001.
35. V. Debaille, A. D. Brandon, Q. Z. Yin, and S. B. Jacobsen. Coupled ^{142}Nd - ^{143}Nd evidence for a protracted magma ocean in Mars. *Nature*, 450:525–528, 2007.
36. V. Debaille, Q.-Z. Yin, A. D. Brandon, and B. Jacobsen. Martian mantle mineralogy investigated by the ^{176}Lu - ^{176}Hf and ^{147}Sm - ^{143}Nd systematics of shergottites. *Earth Planet. Sci. Lett.*, 269:186–199, 2008.
37. J. M. Dohm, V. R. Baker, W. V. Boynton, et al. GRS evidence and the possibility of paleooceans on Mars. *Planet. Space Sci.*, 2008. doi:10.1016/j.pss.2008.10.008.
38. G. Dreibus and H. Wänke. Supply and loss of volatile constituents during the accretion of terrestrial planets. In S. K. Attreya, J. B. Pollack, and M. S. Matthews, editors, *Origin and Evolution of Planetary and Satellite Atmospheres*, pages 268–288. Univ. Arizona Press, 1989.
39. A. M. Dziewonski and D. L. Anderson. Preliminary reference Earth model. *Phys. Earth Planet. Int.*, 25:297–356, 1981.
40. L. T. Elkins-Tanton. Linked magma ocean solidification and atmospheric growth for Earth and Mars. *Earth Planet. Sci. Lett.*, 271:181–191, 2008.
41. L. T. Elkins-Tanton, P. C. Hess, and E. M. Parmentier. Possible formation of ancient crust on Mars through magma ocean processes. *J. Geophys. Res.*, 110:E12S01, 2005.
42. L. T. Elkins-Tanton, E. M. Parmentier, and P. C. Hess. Magma ocean fractional crystallization and cumulative overturn in terrestrial planets: implications for Mars. *Meteorit. Planet. Sci.*, 38:1753–1771, 2003.
43. A. G. Fairén and J. M. Dohm. Age and origin of the lowlands of Mars. *Icarus*, 168:277–284, 2004.
44. A. G. Fairén, J. M. Dohm, V. R. Baker, M. A. de Pablo, J. Ruiz, J. C. Ferris, and R. C. Anderson. Episodic flood inundations of the northern plains of Mars. *Icarus*, 165:53–67, 2003.
45. C. N. Foley, M. Wadhwa, L. E. Borg, P. E. Janney, R. Hines, and T. L. Grove. The early differentiation history of Mars from ^{182}W - ^{142}Nd isotope systematics in the SNC meteorites. *Geochim. Cosmochim. Acta*, 69:4557–4571, 2005.
46. H. V. Frey. Impact constraints on, and a chronology for, major events in early Mars history. *J. Geophys. Res.*, 111:E8S91, 2006.
47. H. V. Frey. Impact constraints on the age and origin of the lowlands of Mars. *Geophys. Res. Lett.*, 33:L08S02, 2006.
48. H. V. Frey and R. A. Schultz. Large impact basins and the mega-impact origin for the crustal dichotomy on Mars. *Geophys. Res. Lett.*, 15:229–232, 1988.
49. G. Ganskow, F. Langenhorst, and D. Frost. Stability of hydrous ringwoodite in the $MgFeSiO_4$ - H_2O system. 5th Colloq. DFG SPP 1115 Münster, p. 8, 2008.
50. A. Ghosh, F. Nimmo, and H. Y. J. McSween. The effect of early accretion and redistribution of ^{26}Al on the thermal evolution of Mars (abstract #2011). *34rd Annual Lunar and Planetary Science Conference. CD-ROM*, 2003.
51. G. A. Glatzmaier. Numerical simulations of mantle convection: Time-dependent, three-dimensional, compressible, spherical shell. *Geophys. Astrophys. Fluid Dyn.*, 43:223–264, 1988.

52. T. V. Gudkova and V. N. Zharkov. Mars: Interior structure and excitation of free oscillations. *Phys. Earth Planet. Int.*, 142:1–22, 2004.
53. A. N. Halliday and T. Kleine. Meteorites and the timing, mechanisms and conditions of terrestrial planet accretion and early differentiation. In D. L. Lauretta and H. Y. McSween, editors, *Meteorites and the Early Solar System II*, pages 775–801. Univ. Arizona Press, Tucson, 2006.
54. A. N. Halliday, H. Wänke, J.-L. Birck, and R. N. Clayton. The accretion, composition and early differentiation of Mars. *Earth Moon Planets*, 96:197–230, 2001.
55. T. Hoogenboom and S. E. Smrekar. Elastic thickness estimates for the northern lowlands of Mars. *Earth Planet. Sci. Lett.*, 248:830–839, 2006.
56. S. B. Jacobsen. The Hf-W isotopic system and the origin of the Earth and the Moon. *Annu. Rev. Earth Planet Sci.*, 32:531–570, 2005.
57. T. Kawamoto. Hydrous phase stability and partial melt chemistry in H_2O-saturated KLB-1 peridotite up to the uppermost lower mantle conditions. *Phys. Earth Planet. Int.*, 143:387–395, 2004.
58. T. Kawamoto. Hydrous phases and water transport in subducting slabs. *Rev. Min. Geochem.*, 62:273–289, 2006.
59. Y. Ke and V. S. Solomatov. Early transient superplumes and the origin of the Martian crustal dichotomy. *J. Geophys. Res.*, 111:E10001, 2006.
60. A. I. S. Kemp, C. J. Hawkesworth, B. A. Paterson, and P. D. Kinny. Episodic growth of the Gondwana supercontinent from hafnium and oxygen isotopes in zircon. *Nature*, 439:580–583, 2006.
61. T. Kleine, K. Mezger, C. Münker, H. Palme, and A. Bischoff. ^{182}Hf-^{182}W isotope systematics of chondrites, eucrites, and martian meteorites: Chronology of core formation and early mantle differentiation in Vesta and Mars. *Geochim. Cosmochim. Acta*, 68:2935–2946, 2004.
62. T. Kleine, K. Mezger, H. Palme, and C. Münker. The W isotope evolution of the bulk silicate Earth: constraints on the timing and mechanisms of core formation and accretion. *Earth Planet. Sci. Lett.*, 228:109–123, 2004.
63. T. Kleine, C. Münker, K. Mezger, and H. Palme. Rapid accretion and early core formation on asteroids and the terrestrial planets from Hf-W chronometry. *Nature*, 418:952–955, 2002.
64. T. Kleine, M. Touboul, B. Bourdon, F. Nimmo, K. Mezger, H. Palme, S. B. Jacobsen, Q.-Z. Yin, and A. N. Halliday. Hf-W chronology of the accretion and early evolution of asteroids and terrestrial planets. *Geochim. Cosmochim. Acta*, 2008. revised version 05/11/2008.
65. A. S. Konopliv, C. F. Yoder, E. M. Standish, D.-N. Yuan, and W. L. Sjogren. A global solution for the Mars' static and seasonal gravity, Mars orientation, Phobos and Deimos masses, and Mars' ephemeris. *Icarus*, 182:23–50, 2006.
66. C. Köstler. *Iterative solvers for modeling mantle convection with strongly varying viscosity.* PhD thesis, Friedrich-Schiller-Univ. Jena, 2009.
67. M. Larin and A. Reusken. A comparative study of efficient iterative solvers for generalized Stokes equations. *Numer. Linear Algebra Appl.*, 15(1):13–34, 2008.
68. A. Lenardic, F. Nimmo, and L. Moresi. Growth of the hemispheric dichotomy and the cessation of plate tectonics on Mars. *J. Geophys. Res.*, 109:E02003, 2004.

69. C. Liebske, B. Schmickler, H. Terasaki, B. T. Poe, A. Suzuki, K.-i. Funakoshi, R. Ando, and D. C. Rubie. Viscosity of peridotite liquid up to 13 GPa: Implications for magma ocean viscosities. *Earth Planet. Sci. Lett.*, 240:589–604, 2005.
70. K. Lodders and B. Fegley. An oxygen isotope model for the composition of Mars. *Icarus*, 126:373–394, 1997.
71. P. Lognonné, D. Giardini, B. Banerdt, et al. The NetLander very broad band seismometer. *Planet. Space Sci.*, 48:1289–1302, 2000.
72. J. Longhi, E. Knittle, J. R. Holloway, and H. Wänke. The bulk composition, mineralogy, and internal structure of Mars. In H. H. Kieffer, B. M. Jakosky, C. W. Snyder, and M. S. Matthews, editors, *Mars*, pages 184–208. Univ. Arizona Press, Tucson, 1992.
73. M. M. Marinova, O. Aharonson, and E. Asphaug. Mega-impact formation of the Mars hemispheric dichotomy. *Nature*, 453:1216–1219, 2008.
74. G. E. McGill and S. W. Squyres. Origin of the Martian crustal dichotomy: Evaluating hypotheses. *Icarus*, 93:386–393, 1991.
75. A. K. McNamara and S. Zhong. Degree-one mantle convection: Dependence on internal heating and temperature-dependent rheology. *Geophys. Res. Lett.*, 32:L01301, 2005.
76. H. J. Melosh. Did an impact blast away half of the martian crust? *Nature Geoscience*, 1:412 – 414, 2008.
77. M. Müller. *Towards a robust Terra code*. PhD thesis, Friedrich-Schiller-Univ. Jena, 2008.
78. G. Neukum, A. T. Basilevsky, M. G. Chapman, et al. Episodicity in the geological evolution of Mars: resurfacing events and ages from cratering analysis of image data and correlation with radiometric ages of martian meteorites. *5th Colloquium DFG Priority Programme SPP 1115: Mars and the Terrestrial Planets*, pages 24–26, 2008.
79. G. Neukum, A. T. Basilevsky, B. A. Ivanov, S. van Gasselt, S. C. Werner, and W. Zuschneid. The geologic evolution of Mars: episodicity of resurfacing events and ages from geologic mapping and cratering analysis of image data. *4th Colloquium DFG Priority Programme SPP 1115: Mars and the Terrestrial Planets*, pages 33–34, 2007.
80. G. Neukum, R. Jaumann, H. Hoffmann, et al. Recent and episodic volcanic and glacial activity on mars revealed by the high resolution stereo camera. *Nature*, 432:971–979, 2004.
81. G. A. Neumann, M. T. Zuber, M. A. Wieczorek, P. J. McGovern, F. G. Lemoine, and D. E. Smith. The crustal structure of Mars from gravity and topography. *J. Geophys. Res.*, 109:E08002, 2004.
82. F. Nimmo. Admittance estimates of mean crustal thickness and density at the Martian hemispheric dichotomy. *J. Geophys. Res.*, 107(E11):5117, 2002.
83. F. Nimmo. Mars's rotating shell. *Nature Geoscience*, 2:7–8, 2009.
84. F. Nimmo, S. D. Hart, D. G. Korycansky, and C. B. Agnor. Implications of an impact origin for the martian hemispheric dichotomy. *Nature*, 453:1220–1223, 2008.
85. F. Nimmo and T. Kleine. How rapidly did Mars accrete? Uncertainties in the Hf - W timing of core formation. *Icarus*, 191:497–504, 2007.
86. F. Nimmo and D. J. Stevenson. Influence of early plate tectonics on the thermal evolution and magnetic field of Mars. *J. Geophys. Res.*, 105(E5):11969–11979, 2000.

87. F. Nimmo and K. Tanaka. Early crustal evolution of Mars. *Annu. Rev. Earth Planet Sci.*, 33:133–161, 2005.
88. C. O'Neill, A. M. Jellinek, and A. Lenardic. Conditions for the onset of plate tectonics on terrestrial planets and moons. *Earth Planet. Sci. Lett.*, 261:20–32, 2007.
89. S. W. Parman. Helium isotopic evidence for episodic mantle melting and crustal growth. *Nature*, 446:900–903, 2007.
90. R. R. Rafikov. The growth of planetary embryos: orderly, runaway or oligarchic? *Astrophys. J.*, 125:942–961, 2003.
91. A. Ramage and A. J. Wathen. Iterative solution techniques for the Stokes and the Navier-Stokes equations. *Int. J. Num. Meth. Fluids*, 19:67–83, 1994.
92. C. C. Reese and V. S. Solomatov. Fluid dynamics of local Martian magma oceans. *Icarus*, 184:102–120, 2006.
93. K. Righter and M. J. Drake. Core formation in Earth's Moon, Mars, and Vesta. *Icarus*, 124:513–529, 1996.
94. J. H. Roberts and S. Zhong. Degree-1 convection in the Martian mantle and the origin of the hemispheric dichotomy. *J. Geophys. Res.*, 111:E06013, 2006.
95. D. C. Rubie, H. Terasaki, Y. Asahara, et al. New constraints on core formation and planetary accretion. 5th Colloq. DFG Priority Programme SPP 1115, Münster,p. 1, 2008.
96. C. Sanloup, A. Jambon, and P. Gillet. A simple chondritic model of Mars. *Phys. Earth Planet. Int.*, 112:43–54, 1999.
97. G. Schubert, S. C. Solomon, D. L. Turcotte, M. J. Drake, and N. H. Sleep. Origin and thermal evolution of Mars. In H. H. Kieffer, B. M. Jakosky, C. W. Snyder, and M. S. Matthews, editors, *Mars*, pages 147–183. Univ. Arizona Press, 1992.
98. G. Schubert and T. Spohn. Thermal history of Mars and the sulfur content of its core. *J. Geophys. Res.*, 95:14095–14104, 1990.
99. N. H. Sleep. Martian plate tectonics. *J. Geophys. Res.*, 99(E3):5639–5655, 1994.
100. D. E. Smith, M. T. Zuber, H. V. Frey, J. B. Garvin, J. W. Head, D. O. Muhleman, G. H. Pettengill, R. J. Phillips, S. C. Solomon, H. J. Zwally, W. B. Banerdt, T. C. Duxbury, M. P. Golombek, F. G. Lemoine, G. A. Neumann, D. D. Rowlands, O. Aharonson, P. G. Ford, A. B. Ivanov, C. L. Johnson, P. J. McGovern, J. B. Abshire, R. S. Afzal, and X. Sun. Mars Orbiter Laser Altimeter: Experiment summary after the first year of global mapping of Mars. *J. Geophys. Res.*, 106:23689–23722, Oct 2001.
101. J. R. Smyth. A crystallographic model for hydrous wadsleyite (β-Mg_2SiO_4): An ocean in the Earth's interior? *Am. Min.*, 79:1021–1024, 1994.
102. F. Sohl, G. Schubert, and T. Spohn. Geophysical constraints on the composition and structure of the Martian interior. *J. Geophys. Res.*, 110:E12008, 2005.
103. F. Sohl and T. Spohn. The interior structure of Mars: Implications from SNC meteorites. *J. Geophys. Res.*, 102(E1):1613–1635, 1997.
104. V. S. Solomatov. Fluid dynamics of a terrestrial magma ocean. In R. M. Canup and K. Righter, editors, *Origin of the Earth and Moon*, pages 323–337. Univ. Arizona Press, Tucson, 2000.
105. V. S. Solomatov and C. C. Reese. Grain size variations in the Earth's mantle and the evolution of primordial chemical heterogeneities. *J. Geophys. Res.*, 113:B07408, 2008.

106. S. C. Solomon, O. Aharonson, W. B. Banerdt, et al. Why are there so few magnetic anomalies in martian lowlands and basins. *Lunar and Planetary Science Conference*, 34:1382.pdf, 2003.
107. T. Spohn. Mantle differentiation and thermal evolution of Mars, Mercury and Venus. *Icarus*, 90:222–236, 1991.
108. T. Spohn. Planetologie. In *L. Bergmann and C. Schaefer, 7: Erde und Planeten*, Lehrbuch der Experimentalphysik, pages 427–525. Walter de Gruyter, 2001.
109. T. Spohn. Planetary evolution and habitability. *European Planetary Science Congress Abstracts*, 3:EPSC2008–A–00602, 2008.
110. T. Spohn, F. Sohl, and D. Breuer. Mars. *Astron. Astrophys. Rev.*, 8:181–236, 1998.
111. K. F. Sprenke and L. L. Baker. Magnetization, paleomagnetic poles, and polar wander on Mars. *Icarus*, 147:26–34, 2000.
112. S. Stanley, L. Elkins-Tanton, M. T. Zuber, and E. M. Parmentier. Mars' paleomagnetic field as the result of a single-hemisphere dynamo. *Science*, 321:1822–1825, 2008.
113. C. Stein, J. Schmalzl, and U. Hansen. The effect of rheological parameters on plate behavior in a self-consistent model of mantle convection. *Phys. Earth Planet. Int.*, 142:225–255, 2004.
114. P. J. Tackley. Self-consistent generation of tectonic plates in time-dependent, three-dimensional mantle convection simulations. Part 1. Pseudoplastic yielding. *Geochem. Geophys. Geosys.*, 1:2000GC000036, 2000.
115. P. J. Tackley. Self-consistent generation of tectonic plates in time-dependent, three-dimensional mantle convection simulations. Part2. Strain weakening and asthenosphere. *Geochem. Geophys. Geosys.*, 1:2000GC000043, 2000.
116. E. Tan, E. Choi, P. Thoutireddy, M. Gurnis, and M. Aivazis. Geoframework: Coupling multiple models of mantle convection within a computational framework. *Geochem. Geophys. Geosys.*, 7:Q06001, 2006.
117. G. J. Taylor, W. Boynton, J. Brückner, et al. Bulk composition and early differentiation of Mars. *J. Geophys. Res.*, 112(E3):E03S10, 2007.
118. R. Trompert and U. Hansen. Mantle convection simulations with rheologies that generate plate-like behavior. *Nature*, 395:686–689, 1998.
119. O. Verhoeven, A. Rivoldini, P. Vacher, et al. Interior structure of terrestrial planets: Modeling Mars' mantle and its electromagnetic, geodetic, and seismic properties. *J. Geophys. Res.*, 110:E04009, 2005.
120. U. Walzer, T. Burghardt, and R. Hendel. Toward a dynamic model of the Martian mantle. 5th DFG Colloq. on Mars SPP 1115 Münster, 28-29 Feb, 2008.
121. U. Walzer and R. Hendel. Time-dependent thermal convection, mantle differentiation, and continental crust growth. *Geophys. J. Int.*, 130:303–325, 1997.
122. U. Walzer and R. Hendel. Mantle convection and evolution with growing continents. *J. Geophys. Res.*, 113:B09405, doi:10.1029/2007JB005459, 2008.
123. U. Walzer, R. Hendel, and J. Baumgardner. The effects of a variation of the radial viscosity profile on mantle evolution. *Tectonophysics*, 384:55–90, 2004.
124. U. Walzer, R. Hendel, and J. Baumgardner. Viscosity stratification and a 3D compressible spherical shell model of mantle evolution. In E. Krause, W. Jäger, and M. Resch, editors, *High Perf. Comp. Sci. Engng. '03*, pages 27–67. Springer, Berlin, 2004.

125. U. Walzer, R. Hendel, and J. Baumgardner. Whole-mantle convection, continent generation, and preservation of geochemical heterogeneity. In W. E. Nagel, D. B. Kröner, and M. M. Resch, editors, *High Perf. Comp. Sci. Engng. '07*, pages 603–645. Springer, Berlin, 2008.
126. W. R. Ward. On planetesimal formation: The role of collective particle behaviour. In R. M. Canup and K. Righter, editors, *Origin of the Earth and Moon*, pages 75–84. Univ. Arizona Press, Tucson, 2000.
127. T. R. Watters, P. J. McGovern, and R. P. Irwin III. Hemispheres apart: The crustal dichotomy on Mars. *Annu. Rev. Earth Planet Sci.*, 35:621–652, 2007.
128. S. J. Weidenschilling. Dust to planetesimals. *Icarus*, 44:172–189, 1980.
129. S. J. Weidenschilling and J. N. Cuzzi. Formation of planetesimals in the solar nebula. In E. H. Levy and J. I. Lunine, editors, *Protostars and Planets III*, pages 1031–1060. Univ. Arizona Press, Tucson, 1993.
130. S. J. Weidenschilling, D. Spaute, D. R. Davis, F. Marzari, and K. Ohtsuki. Accretional evolution of a planetesimal swarm, 2. The terrestrial zone. *Icarus*, 128:429–455, 1997.
131. M. A. Wieczorek and M. T. Zuber. Thickness of the Martian crust: Improved constraints from geoid-to-topography ratios. *J. Geophys. Res.*, 109:E01009, 2004.
132. D. E. Wilhelms and S. W. Squyres. The Martian hemispheric dichotomy may be due to a giant impact. *Nature*, 309:138–140, 1984.
133. W.-S. Yang and J. R. Baumgardner. A matrix-dependent transfer multigrid method for strongly variable viscosity infinite Prandtl number thermal convection. *Geophys. Astrophys. Fluid Dyn.*, 92:151–195, 2000.
134. Q. Z. Yin, S. B. Jacobsen, K. Yamashita, J. Blichert-Toft, P. Télouk, and F. Albarède. A short timescale for terrestrial planet formation from Hf-W chronometry of meteorites. *Nature*, 418:949 – 952, 2002.
135. C. F. Yoder, A. S. Konopliv, D. N. Yuan, E. M. Standish, and W. M. Folkner. Fluid core size of Mars from detection of the solar tide. *Science*, 300:299–303, 2003.
136. M. Yoshida and A. Kageyama. Low-degree mantle convection with strongly temperature- and depth-dependent viscosity in a three-dimensional spherical shell. *J. Geophys. Res.*, 111:B03412, 2006.
137. A. N. Youdin and F. H. Shu. Planetesimal formation by gravitational instability. *Astrophys. J.*, 580:494–505, 2002.
138. K. J. Zahnle, J. F. Kasting, and J. B. Pollack. Evolution of a steam atmosphere during Earth's accretion. *Icarus*, 74:62–97, 1988.
139. V. N. Zharkov and T. V. Gudkova. Construction of Martian interior model. *Solar System Research*, 39(5):343–373, 2005.
140. V. N. Zharkov, T. V. Gudkova, and S. M. Molodensky. On models of Mars' interior and amplitudes of forced nutations. 1. The effects of deviation of Mars from its equilibrium state on the flattening of the core-mantle boundary. *Phys. Earth Planet. Int.*, 172:324–334, 2009.
141. S. Zhong. Differential rotation of lithosphere for one-plate planets and its implications for the Tharsis Rise on Mars. *American Geophysical Union, Fall Meeting, abstract# P43C-1408*, 2008.
142. S. Zhong. Migration of Tharsis volcanism on Mars caused by differential rotation of the lithosphere. *Nature Geoscience*, 2:19–23, 2009.
143. S. Zhong and M. T. Zuber. Degree-1 mantle convection and the crustal dichotomy on Mars. *Earth Planet. Sci. Lett.*, 189:75–84, 2001.

144. M. T. Zuber, S. C. Solomon, R. J. Phillips, et al. Internal structure and early thermal evolution of Mars from Mars Global Surveyor topography and gravity. *Science*, 287:1788–1793, 2000.